dc Conduction Properties of a Model Ethylene–Methacrylic Acid Ionomer

Shoichi Kutsumizu,*,† Yoshio Hashimoto,† Hisaaki Hara,‡ Hitoshi Tachino,‡ Eisaku Hirasawa,‡ and Shinichi Yano†

Department of Chemistry, Faculty of Engineering, Gifu University, Yanagido, Gifu 501-11, Japan, and Technical Center, DuPont-Mitsui Polychemicals Company Ltd., 6 Chigusa-kaigan, Ichihara, Chiba 299-01, Japan

Received August 17, 1993; Revised Manuscript Received January 5, 1994•

ABSTRACT: dc conductivity (σ) in the temperature range from room temperature to 400 K was examined for a zinc(II) complex salt of a poly(ethylene-*co*-5.4 mol % methacrylic acid) (EMAA) ionomer with 1,3-bis(aminomethyl)cyclohexane (BAC), where the neutralization degree by zinc(II) was 60% and the equivalent ratio of BAC to COOH was 0.4. In σ vs the reciprocal of temperature ($1/T$) plots measured in the heating process, a sample aged at room temperature exhibited a bend near 366 K and an anomalous peak near 325 K. The bend corresponds to the melting point of polyethylene crystallites (T_m). Interestingly, the temperature exhibiting the anomalous peak coincided with an order–disorder transition temperature of the ionic clusters (T_i) observed by differential scanning calorimetry (DSC). This peak was not observed in the cooling process from a temperature above T_m, but in the subsequent heating, the peak reappeared; the peak area became larger, and its position shifted to higher temperatures during aging at room temperature. This thermal hysteresis is phenomenologically analogous to that of the T_i peak observed on DSC. From DSC, X-ray scattering, and thermally stimulated depolarization current results, it was concluded that the dc conduction mainly comes from ionic conduction and that the 325 K peak originates from the ionic cluster transition at T_i.

Introduction

It is well-known that polar ionic groups of ionomers interact with each other to sometimes form ionic aggregates in the hydrophobic polymer matrix and that the formation of ionic aggregates improves mechanical properties of ionomers. Hence, the formation and structure of ionic aggregates have been investigated by using various physical techniques such as small-angle X-ray scattering (SAXS), electron microscopy, extended X-ray absorption fine structure (EXAFS), and electron spin resonance (ESR).[1-4] From these studies, several morphological models have been proposed on the structure of ionic aggregates.[5-9]

Dielectric relaxation spectroscopy is a powerful technique for investigating the formation and structure of ionic aggregates, because it can detect the molecular motion of ionomers through the polar ionic groups which exist in the nonpolar hydrophobic polymer matrix. Phillips et al.[10] and we[11,12] studied dielectric relaxations of poly(ethylene-*co*-methacrylic acid) (EMAA) ionomers; the dielectric relaxational behavior well reflects the microphase separation of ionic aggregates from the polymer matrix, i.e. the formation of an ionic cluster phase in Eisenberg's terminology.[9] On the contrary, little attention has been paid to fundamental investigation of dc conduction properties of ionomers.[13-15] This is probably because EMAA ionomers electrically belong to insulators; their dc electrical conductivities usually lie around 10^{-17}–10^{-18} S cm^{-1} at room temperature, although they could show a small increase by increasing the ion content. On the other hand, the conductivity increases by water uptake, and taking advantage of this increase, the development of electro-conductive or antistatic ionomers has been investigated by several researchers.[16]

Very recently, we studied the temperature dependence of dc conductivity (σ) for EMAA ionomers neutralized by Zn(II) and/or 1,3-bis(aminomethyl)cyclohexane [BAC, $C_6H_{10}(CH_2NH_2)_2$] and found an anomalous peak near 325 K, which was related to a structural change inside the ionic clusters.[15] The present work is undertaken to clarify the origin of the anomalous σ peak by investigating dc conduction and the thermally stimulated depolarization current (TSDC) for a model EMAA ionomer, EMAA–0.6Zn–0.4BAC, where 0.6Zn and 0.4BAC mean 60% neutralization by Zn(II) and a 0.4 equivalent ratio of BAC to carboxylic acid of EMAA, respectively. This model ionomer was confirmed to form an ionic cluster phase by SAXS and dielectric studies.[11] The origin of the anomalous peak is discussed in the context of the order–disorder transition model of the ionic cluster phase.[17-19]

Experimental Section

Materials. The starting EMAA polymer was from DuPont-Mitsui Polychemicals Co. Ltd., whose MAA content was 5.4 mol %. Both neutralization of EMAA by Zn(II) and complex formation of the Zn(II) salt with BAC were accomplished by a melt reaction in an extruder at ~470 K, as described previously.[19] IR spectra showed the coordination of BAC to Zn(II) and an absence of isolated free BAC in the sample. The elementary analysis data for EMAA–0.6Zn–0.4BAC were obtained in the Laboratory for Organic Elemental Microanalysis of Kyoto University, giving a result well consistent with its formula (Found: C, 77.4; H, 12.9; N, 0.9. Calcd: C, 78.1; H, 12.8; N, 0.9).

Sheet samples 0.8–0.3 mm thick were prepared by compression-molding the pellet samples at 430 K for 10 min and then quenching to room temperature at a cooling rate of about 30 K/min. Prior to the measurements, the sheet samples were aged at room temperature in a vacuum desiccator for more than 1 month. In this paper, we denote these samples as the dry samples, although they still contained residual water of ca. 0.45 wt %. The residual water was determined from the weight loss of the samples after being vacuum-dried at ca. 450 K for 40 min.

Water-uptake sheets were prepared as follows: The dry sample was gold-deposited on both sides to ensure electrical contact between the surface and electrode for the conductivity measurements and then soaked in water for several days at room temperature. Prior to the measurements, the sample was dried in a desiccator containing silica gel for 1 h at room temperature

† Gifu University.
‡ DuPont-Mitsui Polychemicals Co. Ltd.
• Abstract published in *Advance ACS Abstracts,* February 15, 1994.

0024-9297/94/2227-1781$04.50/0

to remove water on the surface. The amount of absorbed water was estimated from the weight gain.

Measurements. dc conductivity measurements were performed by measuring the current through the sheet sample under a steady constant voltage using a Keithley 610 C electrometer (its sensitivity was ca. 10^{-14} A). To exclude the surface current, a three-terminal electrode system was used as described previously.[20] The samples were circular sheets of 50-mm diameter and 0.25–0.8-mm thickness. The outer diameter of the guarded electrode was 37 mm, and those of the guard electrode and the unguarded electrode were 50 mm, while the inner diameter of the guard electrode was 39 mm. Electrical contact between the electrode and sheet sample was confirmed by the following two methods. (1) In Figures 6, 8, and 10–12, gold electrodes were carefully deposited in vacuo on both sides of the sheet sample, and the gold-deposited sample was aged for more than 40 days at room temperature prior to use. (2) In Figures 5–7 and 9, the sheet sample was lightly pressed to the thickness of a Mylar spacer (0.25 mm thick) by the spring-loaded electrodes made of stainless steel at ca. 393 K above the melting temperature (T_m = ca. 362 K) of polyethylene crystallites under a dry N_2 atmosphere. The sample was also aged for more than 40 days at room temperature. No difference was seen between the data obtained by the above two methods of mounting the samples into the electrodes. dc conduction of EMAA–0.6Zn–0.4BAC nearly obeyed Ohm's law at 295 and 350 K in the range 2.6–20.6 kV/cm of applied electric field. The temperature dependence of dc conductivity was measured at a heating/cooling rate of ca. 0.5 K/min under a dry N_2 atmosphere. The temperature was measured by a calibrated Fe–constantan thermocouple touched with the guard electrode.

TSDC measurements were performed using the same setup as that for dc conductivity described above. A dc electric field of ca. 2.7 KV/cm was applied to the sample at 385 K above T_m, and then the sample was cooled to room temperature at a rate of ca. 1 K/min during applying the field. After the circuit was made short at room temperature, TSDC was measured during heating to 385 K at a rate of ca. 0.6 K/min.

DSC measurements were carried out with a Seiko Denshi DSC-210 differential scanning calorimeter at a heating/cooling rate of 5 K/min under a dry N_2 flow of ca. 40 mL/min. The order–disorder transition temperature of ionic clusters (T_i) and its enthalpy change (ΔH_i), T_m and its enthalpy change (ΔH_m) of polyethylene crystallites, and the crystallization temperature (T_c) were obtained from the DSC data. The degree of crystallinity in the polyethylene region (X_c) was calculated by assuming that the heat of fusion of polyethylene crystallites is 290.4 J/g.

Wide-angle X-ray scattering (WAXS) measurements were performed at room temperature with a Rigaku-Denki Geiger Flex 2024 X-ray generator, using Ni-filtered Cu Kα radiation.

Results and Discussion

Structural Change with Temperature. Figure 1 shows changes in the DSC curve of EMAA–0.6Zn–0.4BAC during aging at room temperature. The sample was quenched after holding for 5 min at 403 K above T_m. The sample stored for more than 1 year at room temperature shows two endothermic peaks at 335 and 362 K, which we assigned[17-19] to an order–disorder transition of the ionic cluster phase (T_i) and the melting of polyethylene crystallites (T_m), respectively. The DSC thermogram of the cooling process after the heating run above T_m only shows an exothermic peak at 323 K, corresponding to recrystallization of polyethylene crystallites (T_c), and a transition associated with the ionic cluster phase is not observed. However, as seen in Figure 1, the T_i peak reappears after aging the sample at room temperature; the ionic cluster transition temperature (T_i) and its enthalpy change (ΔH_i) gradually increase during the aging. In our proposed model,[17-19] this phenomenon is explained as a gradual transformation from disordered ionic clusters to ordered clusters during the aging.

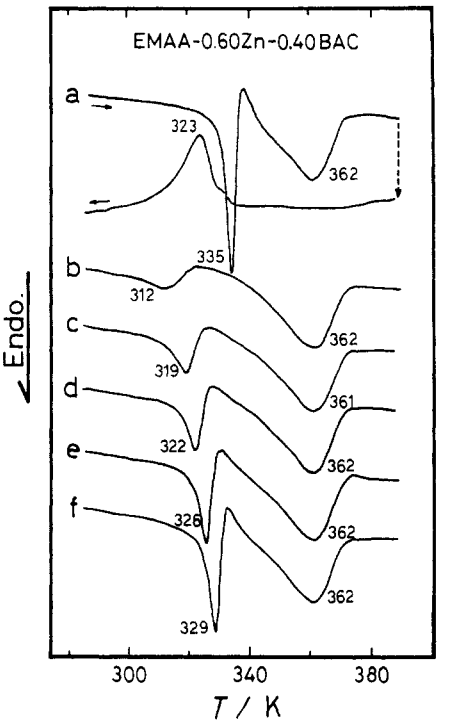

Figure 1. Changes in DSC curve during aging at room temperature for EMAA–0.6Zn–0.4BAC quenched after holding for 5 min at 403 K above T_m. Curve a is for the virgin sample (aged for more than 1 year at room temperature). Curve b is the second heating run just after quenching from 403 K. Curves c–f are for the samples aged for (c) 1 day, (d) 4 days, (e) 11 days, and (f) 37 days, respectively.

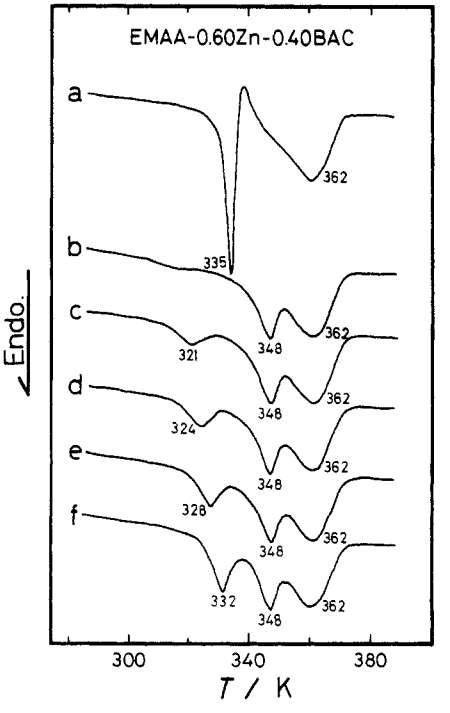

Figure 2. Changes in DSC heating curve during aging at room temperature for EMAA–0.6Zn–0.4BAC quenched after holding for 5 min at 343 K below T_m. Curve a is for the virgin sample. Curve b is the second heating run just after quenching from 343 K. Curves c–f are for the samples aged for (c) 1 day, (d) 3 days, (e) 11 days, and (f) 37 days, respectively.

In order to confirm that the T_i peak is not related to the melting of the so-called quasi-crystallites, we carried out the following experiment: Figure 2 shows changes in the DSC heating curve for the sample quenched after annealing for 5 min at 343 K below T_m. In addition to the T_i and T_m peaks, a new peak is observed at 348 K, 5 K higher

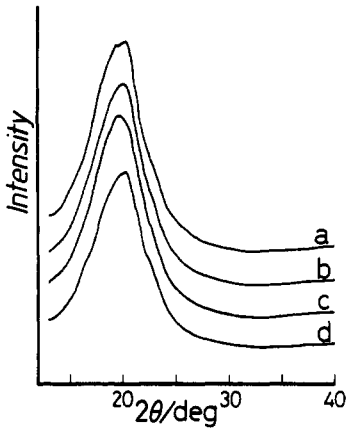

Figure 3. Variation in WAXS pattern during aging at room temperature for EMAA–0.6Zn–0.4BAC quenched from 403 K above T_m. All the patterns were measured at room temperature. Curve a is the pattern immediately measured after quenching from 403 K. Curves b–d are for the samples aged for (b) 1 day, (c) 4 days, and (d) 14 days, respectively.

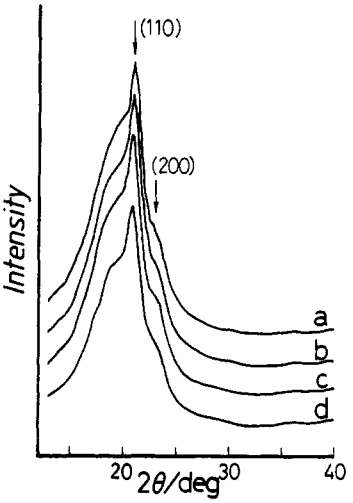

Figure 4. Variation in WAXS pattern during aging at room temperature for EMAA–0.6Zn–0.4BAC quenched from 343 K below T_m. All the patterns were measured at room temperature. Curve a is the pattern immediately measured after quenching from 343 K. Curves b–d are for the samples aged for (b) 1 day, (c) 4 days, and (d) 14 days, respectively.

than the annealing temperature of 343 K. The 348 K peak probably comes from the melting of quasi-crystallites,[18] which are formed by annealing above the crystallization temperature (ca. 323 K). The position and area of this 348 K peak scarcely change during aging at room temperature, but the T_i peak gradually shifts to higher temperatures and the peak area increases, similar to that shown in Figure 1. However, the T_i peak in Figure 2 does not completely revert to that in the original sample: the value of ΔH_i for the sample aged for 37 days was about one-third of that for the original sample. These results suggest that the quasi-crystallites with the melting point of 348 K are not related to the ionic cluster phase and that the presence of quasi-crystallites perturbs the reordering of the ionic cluster phase. The results obtained from Figures 1 and 2 are typical for ethylene ionomers, as we previously reported,[17-19] but certainly offer important information on the origin of the anomalous σ peak.

Figure 3 shows the variation in the X-ray scattering pattern during aging at room temperature for the sample quenched from 403 K above T_m. The pattern shows only a broad halo from the amorphous region and is almost unchanged by aging at room temperature. Therefore, crystallization of polyethylene regions scarcely takes place during the aging. Figure 4 shows the variation in the X-ray scattering pattern during the aging for the sample quenched from 343 K below T_m. All the patterns exhibit a sharp peak at $2\theta = 21°$ and a shoulder at $2\theta = 23°$, which are assigned to (110) and (200) diffractions from polyethylene crystallites, respectively.[21] Therefore, polyethylene crystallites are formed by annealing at 343 K below T_m but not at room temperature. These X-ray scattering results demonstrated that two different annealings at 403 and 343 K, from which the samples were quenched to room temperature, produce a noticeable difference in polyethylene crystallinity. Consequently, the DSC and X-ray scattering results reveal the following facts: (1) Annealing at 343 K below T_m produces quasi-crystallites in the polyethylene region, resulting in the increase of polyethylene crystallinity, while annealing at room temperature does not increase polyethylene crystallinity. (2) Disordered ionic clusters gradually transform into ordered ionic clusters during aging at room temperature, but this transformation is restrained by the existence of quasi-crystallites in the polyethylene region.

dc Conduction Behavior and Its Relationships to the Structure. Figure 5 shows the temperature dependence of the conductivity (σ) for EMAA–0.6Zn–0.4BAC. The σ–$1/T$ curves show a bend near 366 K in the heating and near 334 K in the cooling process, respectively. These bends are related to the melting of polyethylene crystallites and their recrystallization, respectively, because their temperatures almost agree with the T_m (362 K) and T_c (323 K) obtained by DSC, respectively. The σ–$1/T$ plots show a straight line in each temperature range above and below T_m in the heating process and in each temperature range above and below T_c in the cooling process; apparent activation energies (E_a) were estimated to be 2.2 (340 K $< T <$ T_m) and 1.1 eV ($T_m < T$) in the heating and 2.4 (320 K $< T <$ T_c) and 1.0 eV ($T_c < T$) in the cooling process, by using the Arrhenius equation

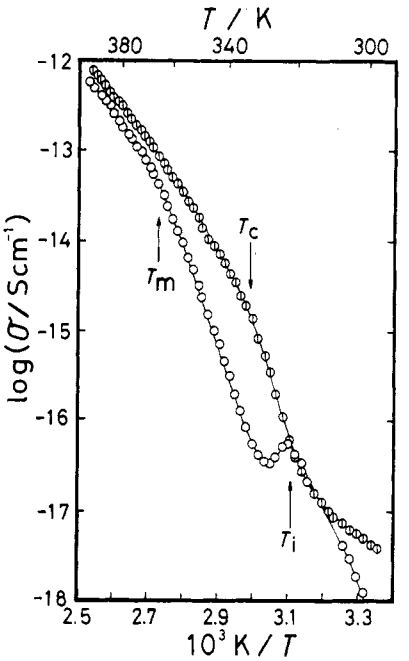

Figure 5. Temperature (T) dependence of conductivity (σ) for EMAA–0.6Zn–0.4BAC: first heating run (○); first cooling run (Φ). T_m = melting point of polyethylene crystallites, T_c = crystallization temperature of polyethylene crystallites, T_i = order–disorder transition temperature of ionic clusters.

$$\sigma(T) = \sigma_0 \exp(-E_a/k_B T) \quad (1)$$

where k_B and σ_0 are the Boltzmann constant and a

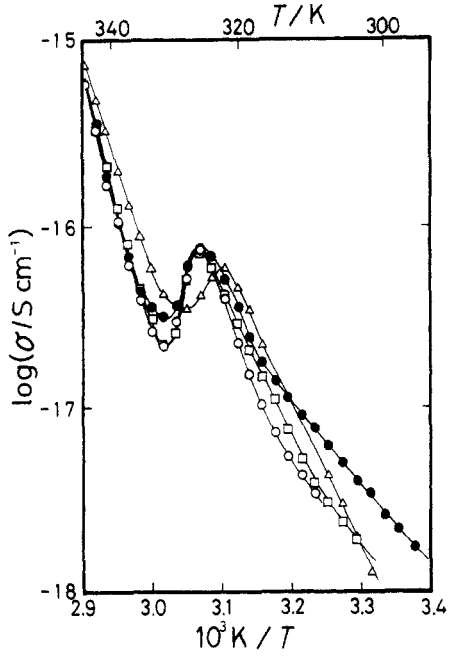

Figure 6. Influence of electrode material and applied voltage on the conductivity (σ)–temperature plot of EMAA–0.6Zn–0.4BAC: gold deposition, electric field 1.1 kV/cm (●); gold deposition, electric field 2.6 kV/cm (□); gold deposition, electric field 3.2 kV/cm (○); heat-press (see Experimental Section), electric field 7.7 kV/cm (△).

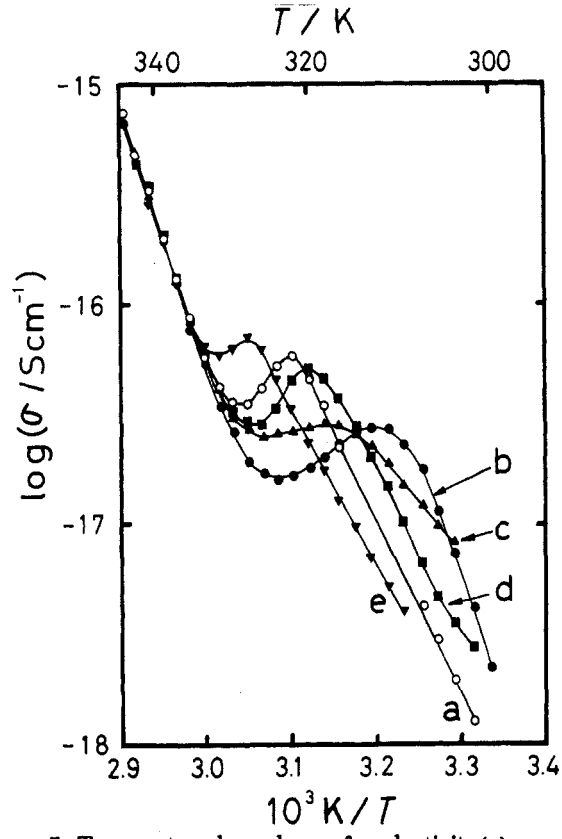

Figure 7. Temperature dependence of conductivity (σ) measured in the heating run for EMAA–0.6Zn–0.4BAC aged at room temperature after quenching from 400 K above T_m: (a) ○, for the sample aged for 47 days at room temperature after quenching from 400 K; (b) ●, the second heating run just after quenching from 400 K; (c) ▲, (d) ■, (e) ▼, after the aging for 1 day, 7 days, and 42 days, respectively. In all the quenching processes, the sample was in short circuit.

proportionality constant, respectively. Another bend seen near 317 K in the cooling process may be due to a glass transition (T_g) of the amorphous polyethylene region, because most polymers show a similar bend near T_g in the Arrhenius plot of σ versus T.[22] It is noted that an anomalous peak is observed at 322 K in the heating process and is depressed in the subsequent cooling process. As shown in Figure 6, this anomalous peak appears regardless of the electrode material and the applied voltage. Therefore, it is obvious that this peak originates from some structural change in this ionomer itself. We postulate that the σ peak originates from the order–disorder transition of the ionic cluster phase at T_i because the temperature exhibiting the σ peak coincides with the DSC T_i (see Figure 1). The σ peak temperature was somewhat influenced by the heating rate of the σ–T measurements, and this will be discussed later (Figure 11).

It is interesting how the difference in thermal treatment influences the appearance of the σ peak. Figure 7 shows the temperature dependence of the conductivity measured in the heating run for the sample aged at room temperature after being quenched from 400 K above T_m. The original sample aged for 47 days at room temperature shows an anomalous peak at 322 K (curve a), as already seen in Figure 5. In the second heating run just after quenching, the anomalous peak is seen at 313 K but is somewhat broad (curve b). As the quenched sample is aged at room temperature, the peak shifts to higher temperatures and becomes sharper. Figure 8 shows the temperature dependence of the conductivity measured in the heating run for the sample quenched from 350 K below T_m. The anomalous peak is also seen near 310 K in the second heating run just after the quenching, but is very broad (curve b). As the sample is aged at room temperature, the peak shifts to higher temperatures and becomes sharper. Nevertheless, the peak is not completely restored to the original one.

The thermal treatment performed in Figure 7 is the same as that in Figures 1 and 3, and the thermal treatment in Figure 8 corresponds to that in Figures 2 and 4. The thermal hystereses of the σ peak seen in Figures 7 and 8 are phenomenologically analogous to those of the DSC T_i peak in Figures 1 and 2, respectively. These results support our postulation that the anomalous σ peak is caused by the ionic cluster transition; the thermal hystereses of the σ peak are closely related to the order–disorder transition at T_i and the slow reordering of the disordered ionic cluster phase during the aging. From Figure 2, it is considered that the thermal cycle between 270 and 350 K below T_m produces quasi-crystallites which melt near 350 K. However, as seen in the inset of Figure 8, the σ–$1/T$ curve does not show any anomaly near 350 K. However, in the σ–$1/T$ curve, the melting of polyethylene crystallites (T_m = ca. 362 K) was seen not as a peak but as a bend. Therefore, it is evident that the σ peak does not come from the melting of quasi-crystallites or crystallites in the polyethylene matrix. In the heating run after quenching from 350 K below T_m, the σ peak appeared but was broader than that after quenching from the melt. In conjunction with the DSC and X-ray results, it is concluded that the reordering of disordered ionic clusters may be perturbed by the presence of quasi-crystallites, resulting in a very broad peak.

It is known that even in short circuit, as-pressed insulating polymers often exhibit thermally activated current peaks, which originate from depolarization of dipoles oriented by a local strain introduced during compression-molding.[23] In fact, an as-pressed EMAA–0.6Zn–0.4BAC often exhibited a current peak near 325 K during heating in short circuit. However, as shown in Figure 9, no current peak was observed near 325 K once

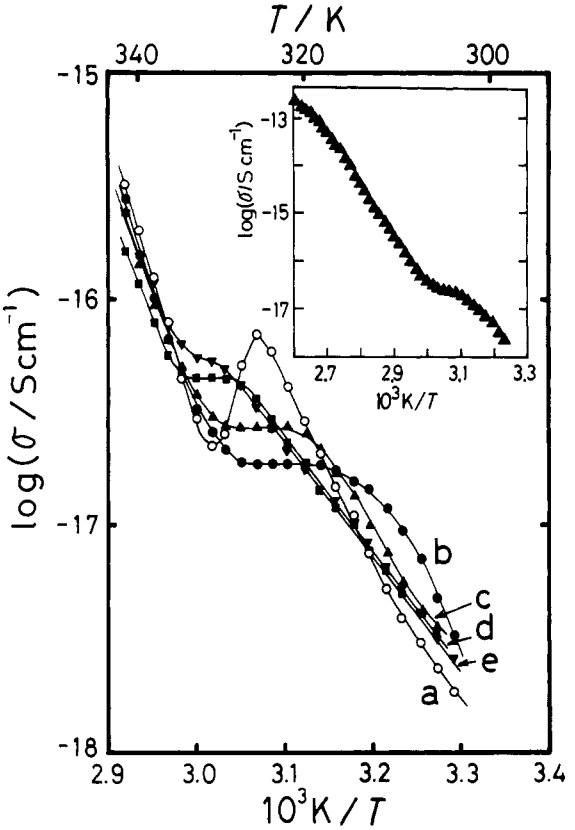

Figure 8. Temperature dependence of conductivity measured in the heating run for EMAA–0.6Zn–0.4BAC aged at room temperature after quenching from 350 K: (a) ○, for the original sample aged for ca. 6 months at room temperature after quenching from ca. 400 K; (b) ●, the second heating run just after quenching from 350 K; (c) ▲, (d) ■, (e) ▼, after aging for 1 day, 10 days, and 44 days, respectively. The inset shows the plot measured up to 388 K for the sample aged for 1 day after quenching from 350 K. In all the quenching processes, the sample was in short circuit.

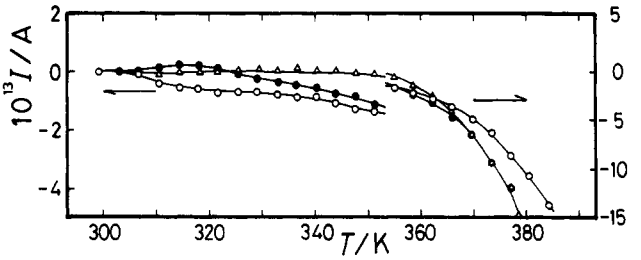

Figure 9. Current (I) vs temperature curves in the heating process for EMAA–0.6Zn–0.4BAC in short circuit. Full circles show plots measured immediately after quenching from 400 K above T_m to room temperature. Triangles and open circles refer to the sample aged at room temperature for 14 and 40 days, respectively, after the quenching.

the sample was heated above T_m, and the I–T curve was unchanged by aging at room temperature. From these results, it is considered that the initial strain is removed by heating the sample above T_m. In Figure 7, the σ peak appears near 325 K although the sample was heated to a temperature above T_m prior to the conductivity measurements. Moreover, the σ peak also appears in the second to fifth heating, where the sample was aged for 1, 7, and 42 days at room temperature after quenching from a temperature above T_m, respectively. These results indicate that the anomalous σ peak is not caused by the internal strain introduced during molding.

Figure 10 shows logarithmic plots of charging current (I) versus time (t) at various temperatures. The decay behavior of charging current apparently depends on temperature. Neglecting small fluctuations probably due

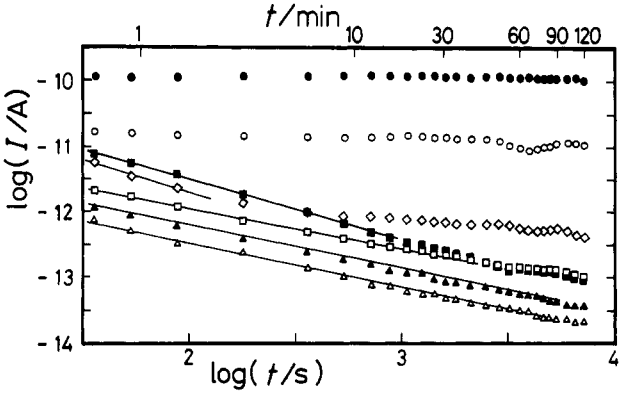

Figure 10. Current (I)–time (t) curves in EMAA–0.6Zn–0.4-BAC at various temperatures under an applied electric field of 3.3 kV/cm: (△) 293 K; (▲) 304 K; (□) 313 K; (■) 323 K; (◇) 333 K; (○) 344 K; (●) 353 K. Each temperature was controlled within ±0.5 K. Current–time curves were also measured at 316 and 328 K but these data are not shown in this figure.

to transient polarizations, the relation of I with t is expressed by

$$I \propto t^{-n} \tag{2}$$

where n is a constant value and expresses a decay rate of I. Below 313 K, n was between 0.6 and 0.7, being nearly equal to that in polyethylene[24] (n = 0.64 at 298 K and n = 0.63 at 320 K). At 323 and 328 K, n was estimated to be 1.1 and 0.9, respectively, and the decay rate is slightly larger than that below 313 K. At temperatures higher than ca. 340 K, I already reaches a constant value within 0.5 min and so is apparently independent of t in Figure 10. The decay behavior of I depends on temperature and abruptly changes near 330 K, which corresponds to T_i of the ionic cluster phase, since T_i is around 330 K (see Figure 1). This abrupt change has often been seen for insulating polymers; insulating polymers exhibit a slow decay of I below T_g, while I quickly reaches an equilibrium value above T_g. This implies that the ionic cluster transition has a glass-transition nature, although the ionic cluster transition is a first-order transition.[17-19] This contradiction may be reconciled by considering that the glass-transition nature of the ionic cluster transition results from softening of ordered ionic clusters which act as a rigid cross-link of the hydrocarbon chains. This interpretation is also supported by the dielectric[10-12] and mechanical[25-27] results; both results showed that in ionomers that form the ionic cluster phase, the α relaxation begins just above T_i, where the α relaxation is attributed to a micro-Brownian segmental motion of long hydrocarbon chains linked to the ionic cluster phase.

We calculated the amount of electric charge carried by the charging current (Q_c) and that by the discharging current (Q_{dc}). Below 328 K, the charging current decayed very slowly and did not reach an equilibrium value even at 120 min after applying the electric field. Assuming the current value at 120 min to be the equilibrium value below 328 K, the Q_c value was almost equal to the Q_{dc} value below 328 K. On the other hand, above 333 K, the Q_c value was twice the Q_{dc} value or more. Therefore, the superposition principle does not hold above 330 K, and this indicates that space charge may accumulate or dissipate above 333 K.

Figure 11 shows temperature dependences of the conductivity (σ) measured at two heating rates and "transient" conductivities at different transient times. The transient conductivities at various temperatures were

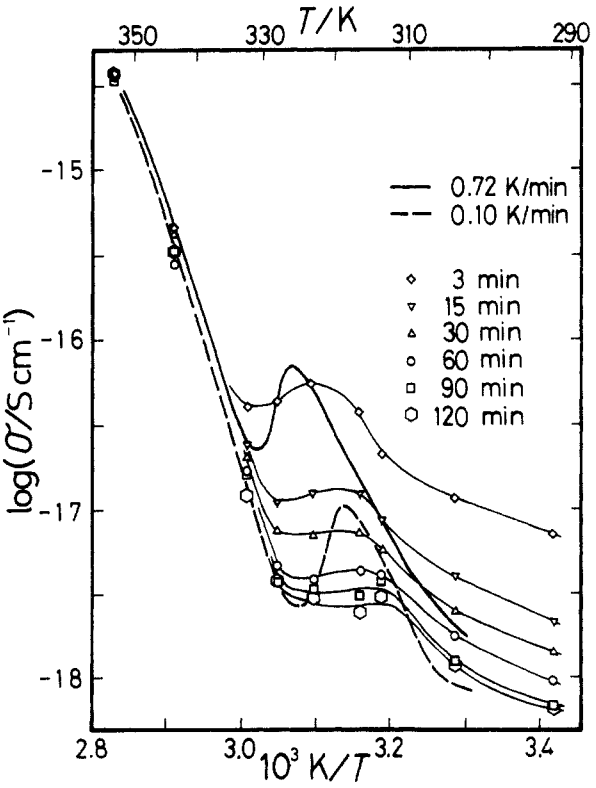

Figure 11. Influence of the heating rate on the conductivity (σ) for EMAA–0.6Zn–0.4BAC: 0.72 K/min (—); 0.10 K/min (- - -). The "transient" conductivities were calculated from the current values at 3 min (◇), 15 min (▽), 30 min (△), 60 min (○), 90 min (□), and 120 min (○) in Figure 10.

calculated from current at various transient times after the electric field was applied. The heating rate scarcely affects the σ–$1/T$ curve above 330 K, but the σ peak temperature shifts to lower temperatures with decreasing heating rate from 0.72 to 0.10 K/min, similar to the DSC data; the DSC T_i decreased from 335 to 327 K with decreasing heating rate from 5 to 0.5 K/min.[28] Therefore, the influence of the heating rate on the T_i peak can be explained by a nonequilibrium phenomenon within the time scale of the measurements. The transient conductivity vs temperature curves also exhibit a broad peak around 323–313 K, and the position gradually shifts to lower temperatures with increasing transient time. Above 333 K, all the transient conductivities fall on the same curve regardless of the transient time and almost agree with the σ–$1/T$ curve measured at the heating rate of 0.72 or 0.10 K/min. From these results, it is concluded that the temperature exhibiting the σ peak depends on the heating rate, because the relaxation time to an equilibrium state is too large.

Effects of Water Absorption on the Conduction Behavior. Figure 12 shows effect of water absorption on the σ–$1/T$ curve. Water absorption increases σ at a given temperature and obscures the σ peak near 325 K. DSC measurements were also performed on EMAA–0.6Zn–0.4BAC samples containing various amounts of water. As the water content increased from 0.45 to 1.1 wt %, T_i and ΔH_i changed from 334 to 322 K and from 29 to 16 J/g, respectively, while X_c showed only a small change from 12 to 16%. These DSC results indicate that water molecules are preferentially incorporated into the ordered ionic cluster phase and destroy some of their structural order, as previously found in EMAA–0.9Na and –0.6Na systems.[29] Hence, the depression of the σ peak with water absorption probably reflects the destruction of an ordered structure within the ionic cluster phase.

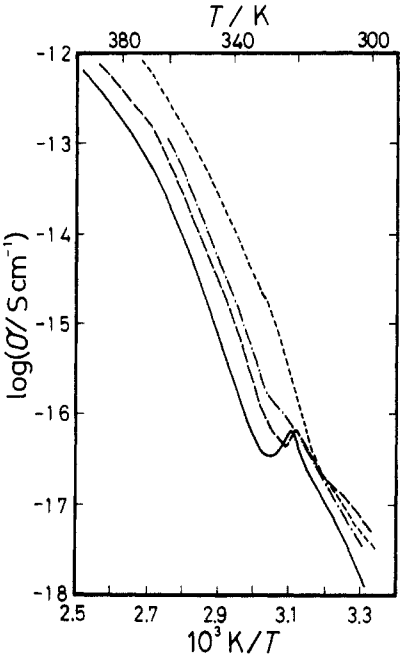

Figure 12. Effects of water absorption on the conductivity (σ) for EMAA–0.6Zn–0.4BAC: dry sample containing 0.45 wt % of the residual water (—); 0.64 (- - -), 0.72 (- · -), and 1.1 wt % (- - -) of water.

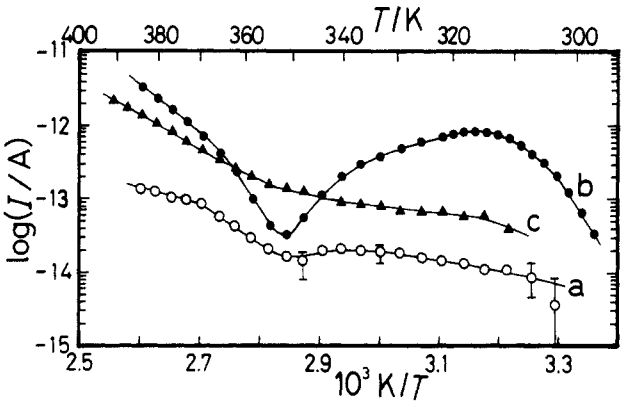

Figure 13. TSDC curves for (a) EMAA and (b) EMAA–0.6Zn–0.4BAC. Curve c is a background current of curve b, i.e the current–temperature plot for EMAA–0.6Zn–0.4BAC cooled from the melt in short circuit. This is due to unavoidable impurity carriers.

TSDC. TSDC curves are shown in Figure 13. EMAA–0.6Zn–0.4BAC showed a peak around 320 K and a current uptake above 355 K, where the current flowed against the direction of the applied field. The former peak may be assigned to the release of charges trapped in the ionic cluster phase, and the latter uptake to the release of charges trapped in the polyethylene crystallites, according to the previous results on other ionomer systems.[30–33] In other words, charged carriers may preferentially be trapped in the disordered ionic clusters and polyethylene crystalline region, when the sample is cooled from the molten state under the applied field. The activation energies, which may correspond to about half of the trapping depth of charged carriers, were estimated to be 2.7 eV below T_i, 2.4 eV between T_i and T_m, and 1.2 eV above T_m, from the initial slopes.[34] The last two values are fairly well consistent with the apparent activation energies for dc conduction (2.2 eV between 340 K and T_m and 1.1 eV above T_m).

Mechanism of dc Conduction. EMAA–0.6Zn–0.4BAC exhibits an anomalous peak near T_i in the σ–$1/T$ curve, and its conduction properties such as the activation energy

of dc conduction and the transient current drastically change near T_i. In other EMAA ionomers that form an ionic cluster phase (e.g. 90% neutralized sodium salt of EMAA), the σ–$1/T$ curve also showed an anomalous peak near T_i.[35] Therefore, the appearance of the σ peak near T_i seems to be a general feature of EMMA ionomers that form the ionic cluster phase.

Before going to further discussion on the mechanism for the appearance of the σ peak, we comment on the nature of carriers for dc conduction in EMAA–0.6Zn–0.4BAC. The major process of the dc conduction is considered to be ionic conduction from the following reasons: (1) EMAA–0.6Zn–0.4BAC contains no conjugated system and hence no π-electrons. (2) The apparent activation energy for dc conduction between 340 K and T_m is relatively high (ca. 2.2 eV); electronic conduction is unrealistic for this large activation energy. (3) As the neutralization by metal cations increases, the polyethylene crystallinity decreases but the conductivity at a given temperature increases.[35] If electronic conduction were the case, a decrease in crystallinity should decrease the conductivity. (4) Water absorption increases the conductivity at a given temperature (see Figure 12). This phenomenon cannot be explained by the electronic conduction process but may be understood by the ionic conduction process. In general, the ionic conduction process is closely connected with both diffusional motions of the polymer chain segments and dissociation of ionic carriers.[36] Absorbed water molecules would act as a plasticizer and would also increase the dissociated ionic carriers, leading to an increase of ionic conductivity.

It is interesting and important why the σ peak appears near T_i. Figure 10 suggests that the space charge effect plays an important role in the dc conduction above ca. 333 K in this ionomer. Moreover, the TSDC results (Figure 13) revealed that charged carriers may be trapped near the surface of disordered ionic clusters, in addition to the interfaces between polyethylene crystallites and amorphous regions. Therefore, it may be reasonable that some of the charged carriers are trapped above T_i at the interfaces between disordered ionic clusters and amorphous regions. From the above assumption, it is expected that the conductivity should decrease discontinuously at T_i, leading to the σ peak.

Another possible mechanism is based on a viewpoint that the σ T_i peak results from a relaxational process. Postulating the order–disorder transition model of ionic clusters,[17-19] either the disordering of permanent electric dipoles or displacement of ions inside the ionic clusters may occur at T_i with increasing temperature. As a result, a transient current peak takes place near T_i, resulting in an apparent peak near T_i in the σ–$1/T$ curve. This mechanism is very similar to the mechanism postulated for an apparent conductivity peak (polarization current) observed near T_g in poly(methyl methacrylate),[24] poly(monochlorotrifluoroethylene),[24] and poly(vinyl chloride).[37,38] In these three polymers, at T_g, the disordering effect of thermal agitation on the permanent electric dipole frozen out below T_g is comparable to the orientational effect of the electric field. In our ionomer system, the T_i is interpreted as a temperature above which the disordering effect of thermal agitation on the backbone chains (i.e. elastic effect) overcomes an ordering by dipole–dipole interaction inside the ionic clusters.[5,17-19]

We propose the above two processes for the explanation of the σ T_i peak, but at present, we cannot determine which process is more dominant. Although the σ T_i peak may have partly a nonequilibrium nature, it is concluded that the appearance of this peak clearly reflects a structural change inside the ionic clusters in this ionomer system.

Acknowledgment. We thank Professor Yasutaka Takahashi of Gifu University for the use of the X-ray diffractometer. S.K. wishes to acknowledge the support of the Ministry of Education, Science, and Culture in Japan (Grant-in-Aid for Scientific Research No. 03750645).

References and Notes

(1) Holliday, L., Ed. *Ionic Polymers*; Applied Sciences: London, 1975.
(2) Eisenberg, A., King, M., Eds. *Ion-Containing Polymers, Polymer Physics*; Academic Press: New York, 1977; Vol. 2.
(3) Pineri, M., Eisenberg, A., Eds. *Structure and Properties of Ionomers*; NATO ASI Series C, Mathematical and Physical Sciences; D. Reidel Co: Dordrecht, The Netherlands, 1987; Vol. 198.
(4) Utracki, L. A., Weiss, R. A., Eds. *Multiphase Polymers: Blends and Ionomers*; ACS Symposium Series 395; American Chemical Society: Washington, DC, 1989.
(5) Eisenberg, A. *Macromolecules* **1970**, *3*, 147.
(6) Macknight, W. J.; Taggart, W. P.; Stein, R. S. *J. Polym. Sci., Polym. Symp.* **1974**, *45*, 113.
(7) Moudden, A.; Levelut, A. M.; Pineri, M. *J. Polym. Sci., Polym. Phys.* **1977**, *15*, 1707.
(8) Yarusso, D. J.; Cooper, S. L. *Macromolecules* **1983**, *16*, 1871.
(9) Eisenberg, A.; Hird, B.; Moore, R. B. *Macromolecules* **1990**, *23*, 4098.
(10) Phillips, P. J.; Macknight, W. J. *J. Polym. Sci., Polym. Phys. Ed.* **1970**, *8*, 727.
(11) Yano, S.; Yamamoto, H.; Tadano, K.; Yamamoto, Y.; Hirasawa, E. *Polymer* **1987**, *28*, 1965.
(12) Yano, S.; Nagao, N.; Hattori, M.; Hirasawa, E.; Tadano, K. *Macromolecules* **1992**, *25*, 368.
(13) Hirota, S. *Rep. Prog. Polym. Phys. Jpn.* **1973**, *13*, 437.
(14) Arai, K.; Eisenberg, A. *J. Macromol. Sci., Phys.* **1980**, *B17*, 803.
(15) Kutsumizu, S.; Hashimoto, Y.; Yano, S.; Hirasawa, E. *Macromolecules* **1991**, *24*, 2629.
(16) Hirasawa, E.; Yano, S. *Preprints of International Symposium on Fine Chemistry and Functional Polymers*; Lanzhou, China, 1990; p 102.
(17) Tadano, K.; Hirasawa, E.; Yamamoto, Y.; Yamamoto, H.; Yano, S. *Jpn. J. Appl. Phys.* **1987**, *26*, L1440.
(18) Tadano, K.; Hirasawa, E.; Yamamoto, H.; Yano, S. *Macromolecules* **1989**, *22*, 226.
(19) Hirasawa, E.; Yamamoto, Y.; Tadano, K.; Yano, S. *Macromolecules* **1989**, *22*, 2776.
(20) Koizumi, N.; Yano, S. *Bull. Inst. Chem. Res., Kyoto Univ.* **1969**, *47*, 320.
(21) Longworth, R. Reference 1, p 134.
(22) For example, see: Saito, S. *Koubunshi* **1968**, *17*, 672 [in Japanese].
(23) For example, see: Sacher, E. *J. Macromol. Sci., Phys.* **1972**, *B6*, 365.
(24) Munick, R. J. *J. Appl. Phys.* **1956**, *27*, 1114.
(25) MacKnight, W. J.; McKenna, L. W.; Read, B. *E. J. Appl. Phys.* **1967**, *38*, 4208.
(26) MacKnight, W. J.; Kajiyama, T.; McKenna, L. *Polym. Eng. Sci.* **1968**, *8*, 267.
(27) Tachino, H.; Hara, H.; Hirasawa, E.; Kutsumizu, S.; Tadano, K.; Yano, S. *Macromolecules* **1993**, *26*, 752.
(28) Kutsumizu, S.; Hashimoto, Y.; Yano, S. Unpublished results.
(29) Kutsumizu, S.; Nagao, N.; Tadano, K.; Tachino, H.; Hirasawa, E.; Yano, S. *Macromolecules* **1992**, *25*, 6829.
(30) Aras, L.; Vanderschueren, J.; Niezette, J.; Vanderschueren, R. *J. Polym. Sci., Polym. Lett. Ed.* **1983**, *21*, 799.
(31) Vanderschueren, J.; Aras, L.; Boonen, C.; Niezette, J.; Corapci, M. *J. Polym. Sci., Polym. Phys.* **1984**, *22*, 2261.
(32) Vanderschueren, J.; Niezette, J.; Corapsi, M.; Yiauakopoulos, G.; Aras, L. Reference 3, p 493.
(33) Suh, K. S.; Damon, D.; Tanaka, J. *IEE Conf. Publ.* **1988**, *289*, 17.
(34) Mort, J., Pfister, G., Eds. *Electronic Properties of Polymers*; John-Wiley & Sons: New York, 1982.
(35) Kutsumizu, S.; Hashimoto, Y.; Sakaida, Y.; Hara, H.; Tachino, H.; Hirasawa, E.; Yano, S. To be published.
(36) Miyamoto, T.; Shibayama, K. *J. Appl. Phys.* **1973**, *44*, 5372.
(37) Ieda, M.; Kosaki, M.; Ohshima, H.; Shinohara, U. *J. Phys. Soc. Jpn.* **1968**, *25*, 1742.
(38) Kosaki, M.; Sugiyama, K.; Ieda, M. *J. Appl. Phys.* **1971**, *42*, 3388.